

A Quantitative Approach to Sequence and Image Weighting

Takeshi Yokoo, MD, PhD,* Won C. Bae, PhD,† Gavin Hamilton, PhD,* Afshin Karimi, MD, PhD, JD,* James P. Borgstede, MD,* Brian C. Bowen, MD, PhD,‡ Claude B. Sirlin, MD,* Christine B. Chung, MD,* John V. Crues, MD,§ William G. Bradley, MD, PhD,* and Graeme M. Bydder, MB, ChB*

Abstract: Weighting is the term most frequently used to describe magnetic resonance pulse sequences and the concept most commonly used to relate image contrast to differences in magnetic resonance tissue properties. It is generally used in a qualitative sense with the single tissue property thought to be most responsible for the contrast used to describe the weighting of the image as a whole.

This article describes a quantitative approach for understanding the weighting of sequences and images, using filters and partial derivatives of signal with respect to logarithms of tissue property values. Univariate and multivariate models are described for several pulse sequences including methods for maximizing weighting and calculating both sequence and image weighting ratios.

The approach provides insights into difficulties associated with qualitative use of the concept of weighting and a quantitative basis for assessing the signal, contrast, and weighting of commonly used sequences and images.

Key Words: magnetic resonance imaging, signal, contrast, weighting, quantification, pulse sequences, filters

(*J Comput Assist Tomogr* 2010;34: 317–331)

The term weighting is used as a label to describe clinical magnetic resonance (MR) sequences and images and a concept to understand the source of signal differences (or contrast) seen on images. The concept is almost always used qualitatively and describes the relationship between (1) MR tissue properties, (2) pulse sequences, and (3) image contrast (Table 1). A pulse sequence or image is said to be weighted for a tissue property (TP; eg, mobile proton density [ρ_m], T_1 , and T_2) when the difference or the change in that property is thought to be the most important source of contrast on images produced by that sequence. Contrast is the difference (or normalized difference) in signal between 2 voxels or groups of similar voxels on an image. It may be intrinsic between normal and abnormal forms of the same tissue or extrinsic when it involves 2 different tissues or fluids.

Although the term weighting is very commonly used in clinical MR, relating image contrast to differences in tissue properties based on the designated weighting of sequence or image may not be straightforward. An image may be described as T_1 -weighted, but only part of it may, in fact, be T_1 -weighted. Other parts may be T_2 -weighted, ρ_m weighted, or have no weighting at all. Even if all the parts of an image are T_1 -

weighted, different tissues and fluids shown on the image may be T_1 -weighted to different degrees, from zero to a maximum. In addition, signal levels are not a particularly useful guide to image weighting. For example, both high and low signal levels may be associated with little or no T_1 or T_2 weighting.

There are other difficulties. The term weighting is applied to both sequences and images, and the weighting of a sequence may differ from that of the image produced by it. For example, ρ_m weighted spin echo (SE) or fast SE sequences are frequently used to produce T_1 -weighted images of the brain.

When a sequence is used to examine a different tissue or fluid, its weighting may change from that for the original tissue or fluid, but the weighting attributed to the sequence in the first application is frequently retained to describe its use in the second application. For example, sequences used to examine the knee are frequently described by the weighting they would have had if they were used to examine the brain. This is unfortunate because the sequence weighting for tendons and ligaments in this situation is usually different from that for gray or white matter.

In other situations, the designated weighting of the sequence may not be the greatest source of contrast. For example diffusion-weighted sequences are often more T_2 -weighted than diffusion weighted. Sometimes the weighting of a tissue or fluid may be of relatively minor importance. Other strategies such as maximizing or minimizing signal from 1 or more tissues may be more significant, and this may be achieved when the sequence weighting for the particular tissue or fluid of interest is very low or zero, although sequences used for this purpose are usually described by their weighting. These problems add an extra dimension of difficulty to a subject that is already complex.

Some of the difficulties with the concept of weighting are longstanding. More than 20 years ago, the American College of Radiology subcommittee on nuclear magnetic resonance nomenclature and phantom development decided not to list the terms T_1 weighting and T_2 weighting in its glossary of MR terms on the grounds that they were ambiguous and confusing.¹ More recently, Elster and Burdette² have described T_1 weighting and T_2 weighting as among the most overused and least understood concepts in MR.

Despite these difficulties, the concept of weighting is one of the most important in MR imaging because it relates contrast on images to differences or changes in tissue properties, and the effects of disease are understood in terms of the changes they produce in these properties. As a result, weighting provides an essential link between observed contrast in disease and the pathologic processes believed to be responsible for the contrast.

The purposes of this article is to describe weighting in quantitative terms (rather than the qualitative approach routinely used in clinical practice) and to show that this approach can be used to assess signal, contrast, and weighting of pulse sequences and images in everyday use. This approach helps resolve many of the difficulties associated with the qualitative use of the concept and provides insights that may not otherwise be apparent.

From the Departments of *Radiology, and †Bioengineering, University of California, San Diego, San Diego, CA; ‡Department of Radiology, MRI Center, University of Miami, Miami, FL; and §Radnet, Inc, Los Angeles, CA. Received for publication May 29, 2008; accepted May 14, 2009.

Reprints: Graeme M. Bydder, MB, ChB, Department of Radiology, University of California, San Diego, 200 W Arbor Dr, San Diego, CA 92103-8226 (e-mail: gbydder@ucsd.edu).

Copyright © 2010 by Lippincott Williams & Wilkins

TABLE 1. Tissue and Fluid Properties, Pulse Sequences, and Image Features

Tissue and Fluid Properties	Pulse Sequences and Their Parameters	Image Features
ρ_m	Spin echo (TR, TE)	S, signal
T_1	Inversion recovery	C_{ab} , absolute contrast, ΔS
T_2	(TR, TI, TE...)	C_{ff} , fractional contrast, $\frac{\Delta S}{S}$
D^* , apparent diffusion coefficient	Spoiled gradient echo (TR, TE, D^* ...)	$CNR = \frac{C_{ab}}{\sigma}, \frac{C_{ff}}{\sigma}$ and σ is the SD of noise
δ , chemical shift		
χ , susceptibility	Pulsed gradient spin echo (TR, TE; ∞)	
Flow		
Perfusion	Balanced steady state free precession (TR, TE, ∞ ...)	

Tissue Properties

As an initial step, it is helpful to review some features of normal values of tissue and fluid properties (eg, $\rho_m, T_1, T_2, \frac{T_2}{T_1}$, and D^*) that are frequently encountered in clinical practice. Normal values of some of these properties cover 3 to 4 orders of magnitude, and so it is helpful to display them on a logarithmic scale that compresses the range and lends itself to the use of fractional differences such as $\frac{\Delta \rho_m}{\rho_m}, \frac{\Delta T_1}{T_1}$, and $\frac{\Delta T_2}{T_2}$ to describe changes.

ρ_m (mobile ρ_m) means the density of protons (or spin density) with T_2 values long enough to be detected with clinical MR systems. In the past, the lowest level of detectability corresponded to a T_2 of approximately 10 ms. Now, the minimum value of T_2 is probably 0.1 or 0.2 ms using ultrashort echo time (UTE) pulse sequences with (nominal) TEs as short as 8 microseconds. The ρ_m of bone is approximately 15% to 20%; meniscus and cartilage, approximately 50% to 70%; soft tissues, approximately 70% to 90%; and relatively pure fluids, very close to 100%. The relatively large difference (approximately 10%) in ρ_m between gray and white matter is because white matter contains more immobile or bound (MR-invisible) protons with very short T_2 values associated with myelin sheaths. The chemical proton densities (which includes all protons) of gray and white matter are similar.

Quite frequently, what is observed are populations of protons with different MR properties. In some areas, the observed signal may reflect the weighted sum of the 2 components. The observed effect may also represent the complex sum including the effect of differences in phase between different components. In addition, the observed TP may not just reflect the property of the tissue but other factors such as inhomogeneity of the magnetic field, pulse sequences that effect different components of the tissue or fluid magnetization in different ways, and magnetization exchange between the different components.

The pattern for mean T_1 values generally follows that for ρ_m , with the shortest mean T_1 values being those of cortical bone (130–200 ms at 1.5 T) and the longest being those of cerebrospinal fluid (CSF) and joint fluid (approximately 4000 ms). Fat has a short T_1 (eg, 250 ms at 1.5 T). Contrast-enhanced blood may have a T_1 as short as 15 to 20 ms.³

In general terms, the pattern of mean T_2 values follows that for ρ_m and T_1 , with T_2 being the shortest for cortical bone (0.4–0.5 ms),⁴ followed by that of tendons, ligaments and menisci (2–8 ms),⁵ soft tissues, and fluids. Because of issues associated with measurement, widely varying values are quoted for the T_2 values of fluids such as CSF extending from 2000 to 3000 ms down to approximately 200 to 300 ms. Values for tissues and fluids and the ratio of $\frac{T_2}{T_1}$ are shown for some common tissues in Table 2 (for 1.5 T).

Mean values of D^* follow the same general pattern but with the important addition of anisotropy, with white matter having a higher D^* when its fibers are parallel to the gradient field than when its fibers are perpendicular to this field.

Values of T_1 tend to increase with static field strength (B_0) approximately to the power of 0.3 or 0.4, whereas T_2 values tend to decrease but to a lesser extent.^{6,7} More detailed values of tissue properties are available in the MR imaging literature. Normal tissues are usually described as showing differences in tissue properties, whereas acquired differences are usually described as changes.

There are also other tissue and fluid properties of importance including flow, perfusion, $T_1\rho$, and stiffness that are not dealt with here for reasons of space.

The SE Sequence (Univariate Signal Model)

The SE Pulse Sequence as a Combination of 3 Filters

The SE sequence consists of a 90-degree pulse, followed by a 180-degree refocusing pulse and a data acquisition at time TE after the 90-degree pulse for conventional SE sequences and TE effective (TE_{eff}) for fast SE sequences, with the cycle repeated after repetition time (TR). It is common to explain contrast in tissue or fluid longitudinal magnetization followed by transverse magnetization plotted against time with the longitudinal magnetization becoming transverse at the time of the 90-degree pulse (Fig. 1). Contrast is represented by the difference between the 2 curves at time TE or TE_{eff} , including the effect of variable refocusing flip angles.⁸ Although this general approach is useful for explaining signal and contrast, it is much less helpful for understanding the weighting of the sequence and the resulting image.

From the Bloch equations, the simplified signals for SE or fast SE sequences is given by

$$S = k\rho_m \left(1 - e^{-\frac{TR}{T_1}} \right) e^{-\frac{TE}{T_2}} \text{ or } S = k\rho_m \left(1 - e^{-\frac{TR}{T_1}} \right) e^{-\frac{TE_{eff}}{T_2}} \tag{1}$$

This can be written as

$$S = kS_{\rho_m} S_T S_{T_2} \tag{2}$$

with

$$S_{\rho_m} = \rho_m, \quad S_T = 1 - e^{-\frac{TR}{T_1}}, \quad S_{T_2} = e^{-\frac{TE}{T_2}}$$

TABLE 2. Values of ρ_m , T_1 , T_2 , $\frac{T_2}{T_1}$, and D^*

ρ_m	
Normal Values, g/mL	
0.0	Air
0.1	Cortical bone and dentine
0.5	Tendons, ligaments, and menisci
0.7	Soft tissues, liver, muscle, and white matter
0.8	Grey matter
1.0	Blood, CSF, urine, joint fluid, and bile
T_1	
Normal Values (1.5 T), ms	
0	Fat
250	Liver and muscle
500	White matter
600	Grey matter
750	Spleen
800	Blood
1200	CSF and urine
4000	
T_2	
Normal Values (1.5 T), ms	
0	Cortical bone and dentine
0.1-1	Tendons, ligaments, and menisci
2-8	Liver and muscle
40	Fat
60	White matter
80	Grey matter
90	Spleen
100	Blood
800	CSF and urine
2000	
T_2/T_1	
Normal Values (1.5 T)	
.001	Bone tendon
.01	Muscle, liver, grey matter, white matter
.1	Fat
1.0	CSF and urine
D^*	
Normal Values, 10^{-3} mm ² /s	
0.0	Fat, white matter (perpendicular)
0.5	Grey matter
0.7	White matter (parallel)
1.0	Liver
1.3-2.3	
3.4	Water

S_{ρ_m} , S_{T_1} , and S_{T_2} are the signals for the separate segments of the equation for each of ρ_m , T_1 , and T_2 . T_1 is scaled relative to TR, and T_2 is scaled related to TE (or TE_{eff}). If instead of plotting signal or magnetization against time as in Figure 1 we plot the signal S_{T_1} against the natural logarithm of T_1 ($\ln T_1$) and S_{T_2} against $\ln T_2$ for the fixed times of the sequence TR and TE (or TE_{eff}), we obtain the curves shown in Figures 2A and B. These are of the form $y = 1 - e^{-\frac{x}{TR}}$ and $y = e^{-\frac{x}{TE}}$ because the variables are T_1 and T_2 for the many different tissues that may be seen on an image rather than the more familiar forms

$y = 1 - e^{-x}$ and $y = e^{-x}$, which describe the recovery of longitudinal magnetization and the decay of transverse magnetization with the variable being time, and T_1 and T_2 are fixed for each tissue as shown for 2 tissues in Figure 1.

The curves shown in Figures 2A and B have the shapes of a low-pass filter (low/short values of T_1 pass are not reduced, whereas high/long values of T_1 are reduced) in Figure 2A and a high-pass filter (high/long values of T_2 pass and low/short values of T_2 are reduced) in Figure 2B. Increase in TR shifts the filter in Figure 2A to the right, similar to a sliding window. Increase in TE or TE_{eff} also shifts the filter in Figure 2B to the right.

We can now see the difference in signal (or contrast) ΔS_{T_1} that results from a difference $\Delta \ln T_1 = \frac{\Delta T_1}{T_1}$ (for small values of Δ) between 2 tissues P and Q (Fig. 3). The contrast depends on the slope of the curve and the size of the fractional difference $\Delta \ln T_1$. In addition to the central sloping region, the curve has high and low signal plateaus where its slope is zero or close to zero. The change or difference in T_1 (or $\Delta \ln T_1$) in these regions produces little or no change in signal and therefore little or no contrast.

The sequence weighting is given by the slope of the curve, and this is shown in Figure 4B. The slope is zero or negative and reaches a minimum (maximum negative value) at the point where $\frac{T_1}{TR} = 1$. This is the point of maximum contrast or weighting. The curve in Figure 4B extends both to the right and to the left of this point, showing that there is significant weighting away from the maximum $\ln T_1$ value and that this is greater to the right (at multiples of $\frac{T_1}{TR}$) than to the left (at fractions of $\frac{T_1}{TR}$).

The same general principles apply to the T_2 curve except that it has a positive slope (Fig. 5). Change in $\ln T_2$ ($\Delta \ln T_2$) produces a change in signal ΔS_{T_2} (or contrast) when this corresponds with a sloping region of the filter. However, little or no change in signal is produced by a change in $\ln T_2$ in regions corresponding to the high or low signal plateaus. The slope of the filter, which is the first partial derivative of signal with respect to $\ln T_2$, shows a maximum value at $\frac{T_2}{TE} = 1$ or $\frac{TE_{eff}}{T_2} = 1$, with the curve greater on the right than on the left (as with the T_1 filter; Fig. 6B).

The final filter for the SE sequence is that for ρ_m . It would be a straight line if a linear x-axis scale was used, but because of the $\ln \rho_m$ scale along the x-axis, it is exponential (Fig. 7).

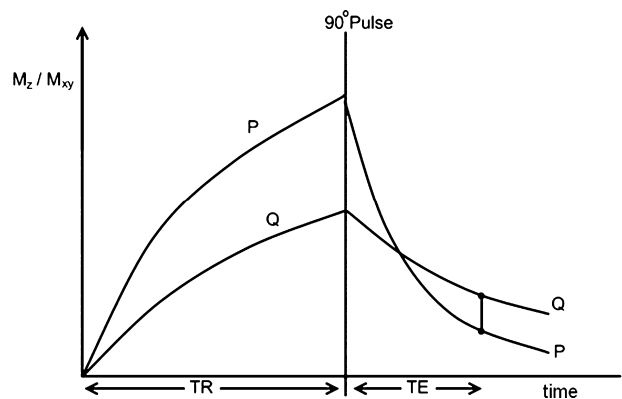


FIGURE 1. Composite diagram for the SE sequence. This shows recovery of the longitudinal magnetization (M_z) for time TR, followed by decay of the transverse magnetization (M_{xy}) for time TE after the 90-degree pulse of the SE sequence, for 2 tissues P and Q. Signal is proportional to M_{xy} at time TE, and the contrast between 2 tissue is proportional to the difference between the 2 curves (vertical line) at time TE.

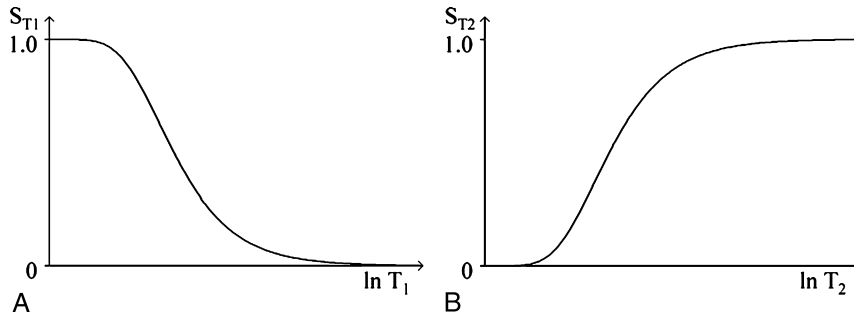


FIGURE 2. Plot of S_{T_1} against $\ln T_1$ (A) and S_{T_2} against $\ln T_2$ (B) for given values of TR (A) and TE (B). The curves have the appearance of low- (A) and high-pass filters (B). Both curves are sigmoid with high and low signal plateaus, as well as the sloping regions between them. Short T_1 values give a high signal in (A), and long T_2 values give a high signal in (B). Increasing TR in A or TE in B both shift the curves to the right.

Mathematical Formalism

In the situation where only one of S_{ρ_m} , S_{T_1} or S_{T_2} differs or is varying (the univariate signal model), the contrast (difference in signal, ΔS) between 2 tissues produced by a small difference in one of the tissue properties, $\Delta\rho_m$, ΔT_1 , or ΔT_2 alone, is given by

$$\begin{aligned} \Delta S_{\rho_m} &= k' \frac{\partial S_{\rho_m}}{\partial \rho_m} \cdot \Delta\rho_m, \Delta S_{T_1} = k' \frac{\partial S_{T_1}}{\partial T_1} \cdot \Delta T_1, \Delta S_{T_2} \\ &= k' \frac{\partial S_{T_2}}{\partial T_2} \cdot \Delta T_2, \end{aligned} \tag{3}$$

where k' is used to designate any constant that is different from k (the symbol \cdot is used to indicate scalar multiplication. It is not the dot product of 2 vectors). Because it is usual to think in fractional changes in tissue properties and because $\frac{\Delta\rho}{\rho} = \Delta \ln \rho_m$, $\frac{\Delta T_1}{T_1} = \Delta \ln T_1$, $\frac{\Delta T_2}{T_2} = \Delta \ln T_2$ (for small Δ), it is useful to use a logarithmic scale for tissue properties and to use the partial derivative of signal with respect to the natural logarithm of each TP rather than with respect to the property itself as shown previously. Using the identity $\frac{\partial f(x)}{\partial \ln x} = x \frac{\partial f(x)}{\partial x}$, this gives

$$\begin{aligned} \Delta S_{\rho_m} &= k' \frac{\partial S_{\rho_m}}{\partial \ln \rho_m} \cdot \frac{\Delta\rho_m}{\rho_m}, \Delta S_{T_1} = k' \frac{\partial S_{T_1}}{\partial \ln T_1} \cdot \frac{\Delta T_1}{T_1}, \\ \Delta S_{T_2} &= k' \frac{\partial S_{T_2}}{\partial \ln T_2} \cdot \frac{\Delta T_2}{T_2}. \end{aligned} \tag{4}$$

We can then see that for each TP, the contrast produced is the product of the partial derivative multiplied by the fractional change in TP.

We can define the sequence weighting sW_{TP} for each TP, with a partial derivative, so that

$$\begin{aligned} sW_{\rho_m} &= k' \frac{\partial S_{\rho_m}}{\partial \ln \rho_m} = \rho_m, sW_{T_1} = k' \frac{\partial S_{T_1}}{\partial \ln T_1} = -\frac{TR}{T_1} e^{-\frac{TR}{T_1}} \\ sW_{T_2} &= k' \frac{\partial S_{T_2}}{\partial \ln T_2} = \frac{TE}{T_2} e^{-\frac{TE}{T_2}}. \end{aligned} \tag{5}$$

For the T_1 component of the sequence, we can put the second derivative $\frac{\partial^2 S_{T_1}}{\partial (\ln T_1)^2} = 0$ to find the point of maximum change in signal (or contrast) that is at $\frac{T_1}{TR} = 1$. We can also put $\frac{\partial^2 S_{T_1}}{\partial \ln T_1 \partial TR} = 0$ to find the TR to maximize weighting for a given T_1 that is also at $\frac{T_1}{TR} = 1$. This gives us the rule for maximizing contrast or weighting by making $\frac{T_1}{TR} = 1$.

A similar result follows for the T_2 filter of the sequence, with $\frac{\partial^2 S_{T_2}}{\partial (\ln T_2)^2} = 0$ and $\frac{\partial^2 S_{T_2}}{\partial \ln T_2 \partial TE} = 0$, which both give $\frac{T_2}{TE}$ (or $\frac{T_2}{TE_{eff}} = 1$). To maximize T_2 -dependent contrast or weighting, we choose $\frac{T_2}{TE}$ (or $\frac{T_2}{TE_{eff}} = 1$).

Absolute Contrast and Fractional Contrast

So far, we have only considered absolute contrast ($C_{ab} = \Delta S$), but fractional contrast ($C_{ab} = C_{fr} = \frac{\Delta S}{S}$ or a variant of this) is also used in MR imaging. To obtain C_{fr} , we divide Equation 5 by S and obtain normalized forms of the sequence weightings:

$$\begin{aligned} sW_{\rho_m/SE/C_{fr}} &= 1, \quad sW_{T_1/SE/C_{fr}} = -\frac{TR}{T_1} \frac{e^{-\frac{TR}{T_1}}}{1 - e^{-\frac{TR}{T_1}}}, \\ sW_{T_2/SE/C_{fr}} &= \frac{TE}{T_2}. \end{aligned} \tag{6}$$

This is only valid if S , S_{ρ_m} , S_{T_1} , and S_{T_2} are not zero or near-zero. The prefix s indicates sequence weighting. The subscripts are given in the order TP/sequence/type of contrast. More detailed notation for weighting is included in Table 3.

Sequence and Image Weightings

We have mainly dealt with sequence weighting, but image weighting is the product of the sequence weighting and the fractional change in TP (Figs. 3 and 5), so the image weightings (iW) for absolute contrast (C_{ab}) are

$$\begin{aligned} iW_{\rho_m/SE/C_{ab}} &= \rho_m \cdot \frac{\Delta\rho_m}{\rho_m}, \\ iW_{T_1/SE/C_{ab}} &= -\frac{TR}{T_1} e^{-\frac{TR}{T_1}} \cdot \frac{\Delta T_1}{T_1}, \\ iW_{T_2/SE/C_{ab}} &= \frac{TE}{T_2} e^{-\frac{TE}{T_2}} \cdot \frac{\Delta T_2}{T_2}; \end{aligned} \tag{7}$$

and for fractional contrast (C_{fr}),

$$\begin{aligned} iW_{\rho_m/SE/C_{fr}} &= 1 \cdot \frac{\Delta\rho_m}{\rho_m}, \\ iW_{T_1/SE/C_{fr}} &= -\frac{TR}{T_1} \frac{e^{-\frac{TR}{T_1}}}{1 - e^{-\frac{TR}{T_1}}} \cdot \frac{\Delta T_1}{T_1}, \\ iW_{T_2/SE/C_{fr}} &= \frac{TE}{T_2} \cdot \frac{\Delta T_2}{T_2}. \end{aligned} \tag{8}$$

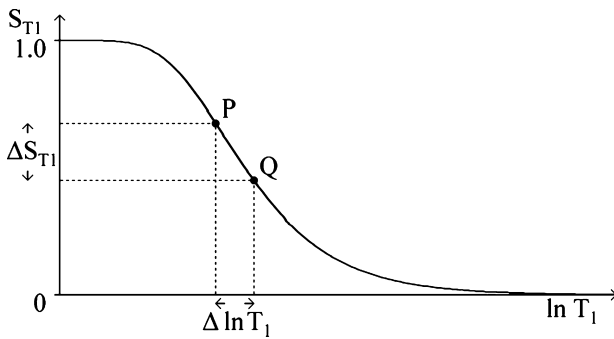


FIGURE 3. Relationship between change in $\ln T_1$ ($\Delta \ln T_1 = \frac{\Delta T_1}{T_1}$ for Δ small) and change in signal (or contrast; S_{T_1}). The difference $\Delta \ln T_1$ produces a change in signal ΔS_{T_1} in a region where the curve is sloping. Change in $\ln T_1$ would produce little or no signal difference (or contrast) in regions corresponding with either the high or the low signal plateaus of the curve.

As before, the univariate model means that we are only dealing with difference or change in one of S_{ρ_m} , S_{T_1} or S_{T_2} at a time, with the other 2 signal functions constant.

For change in T_1 alone, we want $S_{T_2} = e^{-\frac{TE}{T_2}}$ to be constant. If $\frac{T_2}{TE}$ is high as for long values of T_2 and short TEs, S_{T_2} is nearly equal to 1 on the right side of the T_2 filter (Fig. 2B) and therefore constant or nearly constant. If in addition $\frac{\Delta \rho_m}{\rho_m} = 0$, so that only S_{T_1} changes, we can use the univariate model where maximum contrast is achieved at $\frac{T_1}{TR} = 1$. If we are interested in the change in T_2 alone, we want S_{T_1} to be constant and approximately equal to 1 ($\frac{T_1}{TR}$ low, T_1 short), with $\frac{\Delta \rho_m}{\rho_m} = 0$. Then with only S_{T_2} changing, we can use the univariate model for T_2 changes and maximize weighting using the rule $\frac{T_2}{TE}$ or $\frac{T_2}{T_{eff}} = 1$. Pulse sequences are frequently designed to minimize the weighting of one of S_{T_1} or S_{T_2} and maximize the

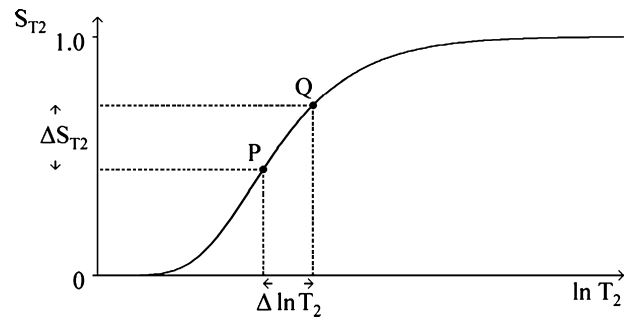


FIGURE 5. Plot of S_{T_2} against $\ln T_2$ for 2 tissues, P and Q. The difference $\Delta \ln T_2$ produces a difference in signal (or contrast; ΔS_{T_2}) when it corresponds with a sloping region of the curve. Little or no difference in signal would be produced by $\Delta \ln T_2$ if it was opposite either the upper or the lower flat regions of the curve.

other, and quite often, $\frac{\Delta \rho_m}{\rho_m}$ is very small or zero. In these circumstances, the univariate model provides a reasonable approach.

The SE Sequence (Multivariate Signal Model)

In the previous section, we dealt with the situation where only 1 of S_{ρ_m} , S_{T_1} , or S_{T_2} varied. However, the more general situation is where all 3 tissue properties, ρ_m , T_1 , and T_2 , differ or change. This is treated in the same general way as for the univariate model, but instead of deriving functions for change of each TP alone, we derive a weighting ratio that is the ratio of the individual weightings to the sum of the magnitudes of all the weightings. This measure includes all 3 properties and quantifies the contribution each property makes to the overall sequence or image weighting.

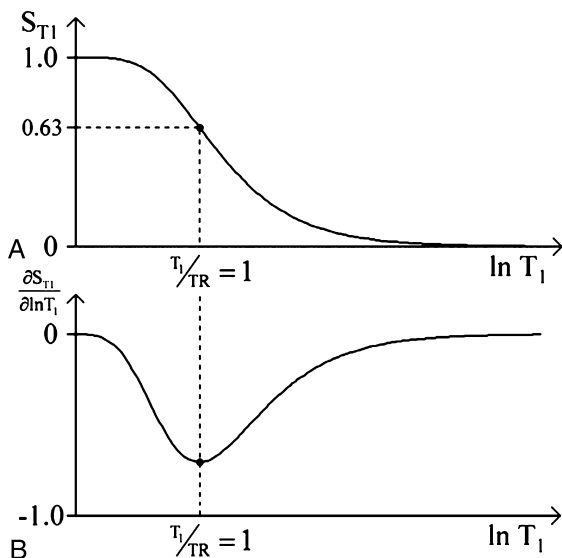


FIGURE 4. Plot of S_{T_1} against $\ln T_1$ (A) and $\frac{\partial S_{T_1}}{\partial \ln T_1}$ against $\ln T_1$ (B). The slope of curve (A) is shown in (B) where it is zero or negative. It is the sequence weighting. The slope reaches a maximum negative value at $\frac{T_1}{TR} = 1$, which is at $1 - e^{-1} = 63\%$ of the maximum signal in (A). The curve of $\frac{\partial S_{T_1}}{\partial \ln T_1}$ (B) is flatter and extends further to the right of the point of maximum slope compared with the left of this point. The sequence weighting is greater at multiples of $\frac{T_1}{TR}$ than at fractions of $\frac{T_1}{TR}$.

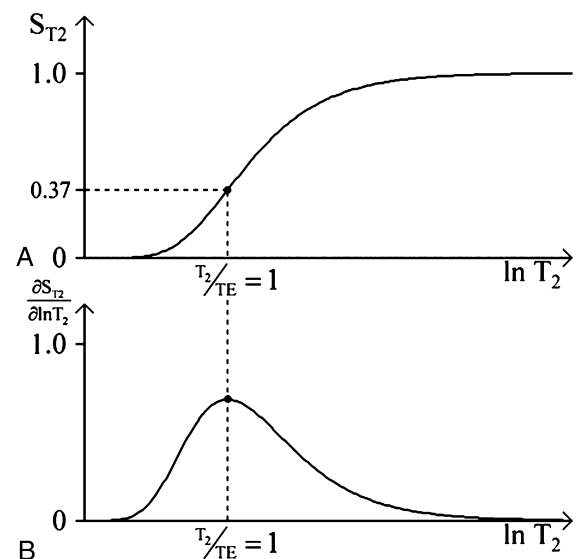


FIGURE 6. Plot of S_{T_2} against $\ln T_2$ (A) and $\frac{\partial S_{T_2}}{\partial \ln T_2}$ against $\ln T_2$ (B). The slope of the curve in (A) is shown in (B). It is zero or positive. It goes through a maximum at $\frac{T_2}{TE} = 1$ where the signal level is 37% of the maximum in (A). The curve is flatter and extends more to the right of the point of maximum slope than it does to the left of this point.

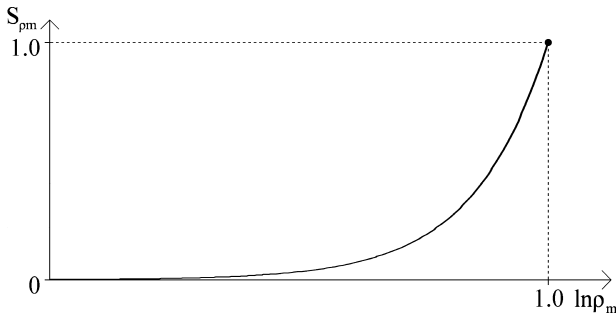


FIGURE 7. Plot of S_{ρ_m} against $\ln \rho_m$. The logarithmic scale compresses high values of ρ_m , and so the curve is steeper on the right.

From Equation 2, providing that none of S , S_{ρ_m} , S_{T_1} , and S_{T_2} are zero or near-zero, we can define the sequence weighting ratio sW (which is the relative contribution of each TP to the overall sequence weighting) as

$$sW_{SE}(\rho_m : T_1 : T_2) = \left(1 : -\frac{TR}{T_1} \frac{e^{-\frac{TR}{T_1}}}{1 - e^{-\frac{TR}{T_1}}} : \frac{TE}{T_2} \right) \quad [9]$$

For the corresponding image weighting ratio, $iW_{SE}(\rho_m : T_1 : T_2)$, we simply multiply each component of the sequence weighting ratio by the relevant fractional change in TP, $\frac{\Delta \rho_m}{\rho_m}$, $\frac{\Delta T_1}{T_1}$ and $\frac{\Delta T_2}{T_2}$ so that

$$iW_{SE}(\rho_m : T_1 : T_2) = \left(1 \cdot \frac{\Delta \rho_m}{\rho_m} : -\frac{TR}{T_1} \frac{e^{-\frac{TR}{T_1}}}{1 - e^{-\frac{TR}{T_1}}} \cdot \frac{\Delta T_1}{T_1} : \frac{TE}{T_2} \cdot \frac{\Delta T_2}{T_2} \right) \quad [10]$$

Within the limits proscribed (no zero or near-zero signals), this describes the contribution of each TP to image weighting in quantitative terms. The total image contrast is the sum of the image weightings for each TP. For the non-zero values described previously, the weighting ratios are independent of the type of contrast, whether absolute (C_{ab}) or fractional (C_{fr}).

The contribution of all tissue filters to image weighting is shown in Figure 8. The fractional difference in each TP, $\frac{\Delta \rho_m}{\rho_m}$, $\frac{\Delta T_1}{T_1}$, and $\frac{\Delta T_2}{T_2}$ is multiplied by the slope for each filter to give the difference in signal between 2 tissues or fluids P and Q (or the contrast ΔS_{ρ_m} , ΔS_{T_1} , and ΔS_{T_2}) produced by each TP. Signals for each TP are multiplied together to give the overall signal for each of P and Q. The difference or contrast between them is shown in the center of the figure. The image weighting ratio $iW(\rho_m : T_1 : T_2)$ can be calculated from the normalized partial derivatives and the fractional differences in tissue properties as shown in the lower part of Figure 8.

Table 4 shows a worked example for an SE sequence based on the data for white and gray matters of the brain from Hendrick⁹ for a T_1 -weighted image obtained at 1.5 T. Normalizing by the magnitude of the signals and using percentages, the sequence weighting ratio $sW_{SE}(\rho_m : T_1 : T_2)$ is (51 : -30 : 19). In qualitative terms, the sequence would be described as ρ_m

weighted (because ρ_m is the greatest source of contrast), but the image weighting ratio, $iW_{SE}(\rho_m : T_1 : T_2)$ is (27 : -61 : 12). This shows that the image would be described as T_1 -weighted using the qualitative approach of naming the sequence by the TP which is the main source of contrast. Thus, in qualitative terms, a ρ_m -weighted sequence has been used to produce a T_1 -weighted image. The greater ρ_m weighting of the sequence is overcome by the greater fractional difference in T_1 to give the greater T_1 weighting on the image. The magnitude of

$$f(x) = \frac{TR}{T_1} \frac{e^{-\frac{x}{T_1}}}{1 - e^{-\frac{x}{T_1}}}$$

is less than 1 for finite values of $\frac{T_1}{TR}$, so from Equation 9, SE sequences cannot be T_1 -weighted (in qualitative terms) because the T_1 weighting is always less than (or at most, equal to) the ρ_m weighting of 1.

A variant of the fast SE technique is half-Fourier acquisition single-shot turbo SE or single-shot fast SE where data obtained at multiple different TEs are combined, and conjugate symmetry is exploited to map k -space. The single-shot approach means that the sequence can be described as having an infinite TR with, for example, TR 5 to 6 times that of the longest T_1 , for example, 22.5 seconds (vs the T_1 of CSF of 4.2 seconds). This maximizes the T_1 -dependent signal and reduces the T_1 weighting to zero or near-zero for all tissues and fluids. As a result, fat (short T_1) and fluid (very long T_1) show similar high signal levels and have little or no T_1 weighting. The typical sequence (eg, $TE_{eff} = 80$ ms) is T_2 -weighted for brain but ρ_m weighted for bile or urine when used for MR cholangiopancreatography or angiography. The intrinsic contrast (difference in signal from the normal value) is less important than the extrinsic contrast (difference in signal from different surrounding tissues or fluids) in these later 2 situations.

Although many of the contrast properties of the fast SE sequence can be modeled using TE_{eff} instead of TE, several effects arise from the succession of inversion pulses used in the fast SE sequence. The inversion pulses used for data acquisition in one slice are off-resonance pulses for other slices. These pulses may partly saturate the magnetization of the bound nuclei and so shorten the observed T_1 and reduce the observed longitudinal magnetization in the free pool. These effects can be modeled by using the observed ρ_m and observed T_1 in Figure 8.

TABLE 3. Notation for Weighting

1. TP, for example, ρ_m , T_1 , and T_2 , or F (full, for all tissue properties)
2. The TP is underscored if it is the only TP that varies as with the univariate model. There is an option for each TP to be absolute or fractional. Because only fractional tissue properties are used in this article, this difference is not specified
3. Sequence (SEQ), for example, SE (or fast SE), IR, PGSE, SGE, partial sequence (form of MP, etc), or other filter. There are 2 options for the partial derivative, that is, linear or logarithmic. We have used logarithmic throughout and so do not distinguish between these 2 options
4. C_{ab} and C_{fr} are the absolute (ab) and fractional (fr) contrast options s or i is sequence or image weighting options, respectively
5. Sequence and image weighting ratios are shown in the form $sW_{SEQ}(TP_1 : TP_2 : TP_3 : \dots)$ or $iW_{SEQ}(TP_1 : TP_2 : TP_3 : \dots)$, where $TP_1, 2, \dots$ are different tissue properties
6. Other forms of weighting, for example, acquisition or post acquisition, can be indicated by a prime superscript, for example, W'

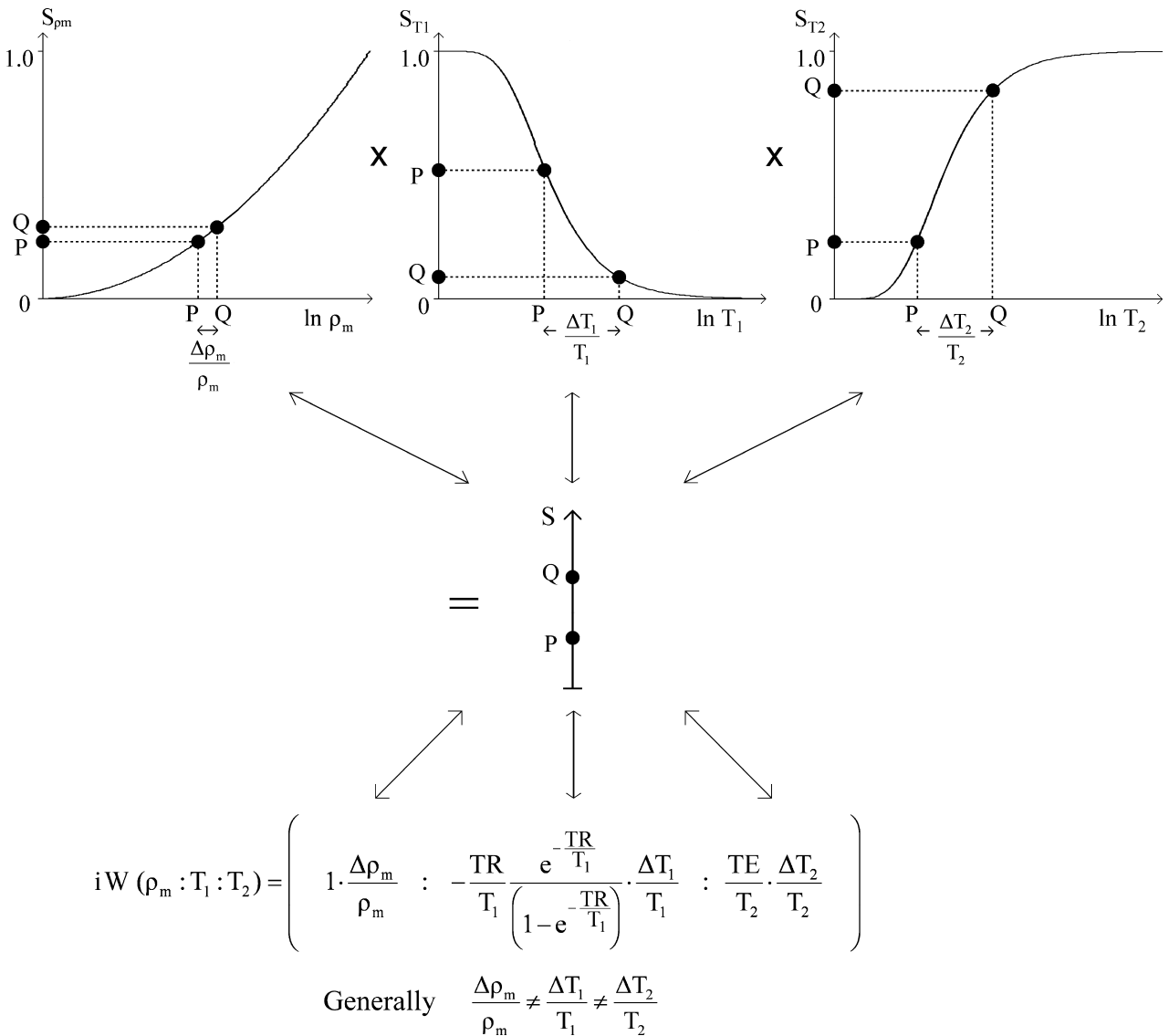


FIGURE 8. Sequences of SE and fast SE and image weighting for 2 tissues, P and Q. This shows how the fractional differences in each TP, $\frac{\Delta\rho_m}{\rho_m}$, $\frac{\Delta T_1}{T_1}$, and $\frac{\Delta T_2}{T_2}$, are multiplied by the slopes of each filter in turn to give the signals for P and Q along the respective S_{ρ_m} , S_{T_1} , and S_{T_2} y-axes in the top row. These signals are then multiplied together to give the overall signals and contrast (difference in signal) shown on the S-axis (y-axis) at the center. The corresponding calculations for the image weighting ratio $iW(\rho_m : T_1 : T_2)$ are shown below where each normalized partial derivative is multiplied by the corresponding fractional change in TP to give the relative contributions of each TP to the contrast between P and Q shown on the y-axis at the center of the image.

The Inversion Recovery Sequence

The inversion recovery (IR) sequence has 2 components controlling T_1 weighting. One, TR is similar to the situation for the SE sequence, and the other follows the inversion pulse. If TR is much greater than the tissue T_1 , the first T_1 filter allows virtually full recovery of the tissue longitudinal magnetization, and the overall T_1 is controlled by the inversion filter of the sequence for which the signal equation is

$$S_{T_1} = 1 - 2e^{-\frac{TI}{T_1}}, \tag{11}$$

where TI is the inversion time. The S_{T_2} component is the same as for the SE or fast SE sequence.

In the first part of this section, we consider the common long TR version of the IR sequence. The T_1 filter for this sequence has twice the range (from +1 to -1) and twice the slope of the corresponding segment of the SE sequence (Fig. 9A). It also passes through zero with a null point where $(1 - 2e^{-\frac{TI}{T_1}}) = 0$, and $\frac{TI}{T_1} = 1.44$. Images can be reconstructed in either phase-sensitive (Fig. 9A) or magnitude form, where the signal beyond the null point is reflected across the x-axis (Fig. 9B). In the later case, the magnitude of the signal is the same, but the sign is positive (rather than negative).

We can illustrate the 3 main classes of the long TR-IR sequence¹⁰ by starting with a short TI and increasing this parameter using white and gray matters as fixed reference tissues. In Figure 10A, we have a short τ inversion recovery (STIR)

TABLE 4. Normal White and Gray Matter, Worked Example (SE_{TR/TE} = 600/20 ms Sequence)

	ρ_m	T_1	T_2
White matter	0.61 g/mL	510 ms	67 ms
Gray matter	0.69 g/mL	760 ms	77 ms
TP fractional difference (relative to the white matter)	$\frac{\Delta\rho_m}{\rho_m} = \frac{0.08}{0.61} = 13\%$	$\frac{\Delta T_1}{T_1} = \frac{250}{510} = 49\%$	$\frac{\Delta T_2}{T_2} = \frac{10}{67} = 15\%$
Signal S _{TP} (% maximum signal)	$S_{\rho_m} = \rho_m = 61\%$	$\frac{T_1}{TR} = 0.85$ $S_{T_1} = (1 - e^{-\frac{TR}{T_1}}) = 69\%$	$\frac{T_2}{TE} = 0.30$ $S_{T_2} = e^{-\frac{TE}{T_2}} = 74\%$
Sequence weighting, sW _{TP/SE/C_{fr}}	sW _{ρ_m/SE/C_{fr}} = 100%	sW _{T_1/SE/C_{fr}} = $\frac{TR}{T_1} = \frac{e^{-\frac{TR}{T_1}}}{(1 - e^{-\frac{TR}{T_1}})} = -36\%$	sW _{T_2/SE/C_{fr}} = $\frac{TE}{T_2} = 22\%$
Sequence weighting ratio, sW _{SE} ($\rho_m:T_1:T_2$)	51%	-30%	19%
Image weighting, iW _{TP} = sW _{TP} • $\frac{\Delta TP}{TP}$	iW _{ρ_m} = sW _{ρ_m} • $\frac{\Delta\rho}{\rho} = 51 \times 13 = 663$	iW _{T_1} = sW _{T_1} • $\frac{\Delta T_1}{T_1} = -30 \times 49 = 1470$	iW _{T_2} = sW _{T_2} • $\frac{\Delta T_2}{T_2} = 19 \times 15 = 285$
Image weighting ratio, iW _{SE} ($\rho_m:T_1:T_2$)	27%	-61%	12%

sequence with the white matter signal less than that of the gray matter. In Figure 10B, we have a medium TI sequence with the white matter signal greater than that of the gray matter, and in Figure 10C, we have a long TI or T₂-fluid-attenuated inversion recovery (FLAIR) sequence with both the white and gray matter high signals. The signal from the white matter is slightly greater than that from the gray matter.

In the multivariate approach, the positive contrast of the STIR sequence using magnitude reconstruction is combined with the positive contrast of the ρ_m and T₂ filters to give additive high contrast. With the medium TI sequence, TE or TE_{eff} is usually reduced to minimize the opposed T₂ weighting. The T₁ contrast is usually high. With the T₂-FLAIR sequence, the slightly greater signal from the white matter compared with that from the gray matter tends to counter the opposed contrast from ρ_m , giving a net low contrast background for the brain against

which high signal lesions produced by the sequences with heavy T₂ weighting and the increased T₂ of lesions can be seen. Although the T₂-FLAIR sequence has heavy T₂ weighting, it also often has a 10–20% residual opposed T₁-weighting. Plots of S_{T₁}, the first and normalized first partial derivatives, are shown in Figure 11.

It is possible to shorten TR so that both TR and TI affect T₁ contrast. One example of this shorter TR-IR sequence is the balanced inversion recovery (BIR) sequence with $\frac{TR}{TI} = 2$. This is similar to the T₁-FLAIR sequence.¹¹ The filter for the BIR sequence is shown in Figure 12, where it lies between that of the long TR-IR sequence and that of an SE Sequence. The BIR/T₁-FLAIR sequence typically produces contrast that is greater than that of the SE sequence (ie, it has greater slope) but less than that of the long TR-IR. The sequence has maximum weighting at $\frac{TR}{TI} = 0.8$.

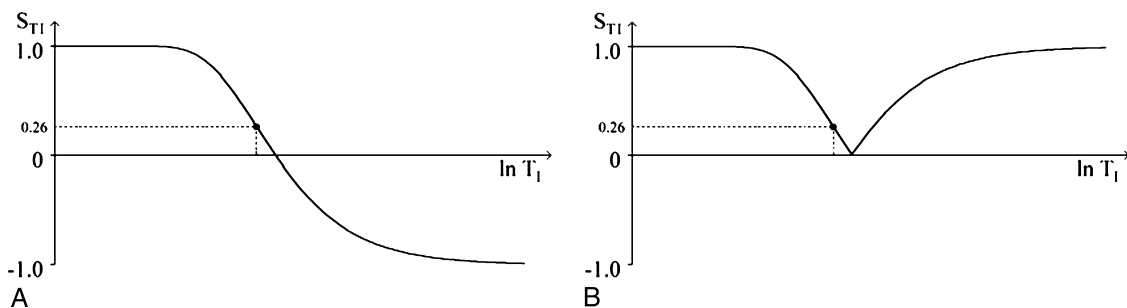


FIGURE 9. Long TR-IR sequence T₁ filters with phase-sensitive (A) and magnitude reconstructions (B). The curve in (A) has high and low signal plateaus with a sloping region between. It has twice the range (+1 to -1) and twice the slope of the corresponding SE T₁ filter. The curve in (B) is the same as that in (A) up to the zero or null point. Beyond this, the curve in B is a mirror reflection across the x-axis (lnT₁) of the curve in (A).

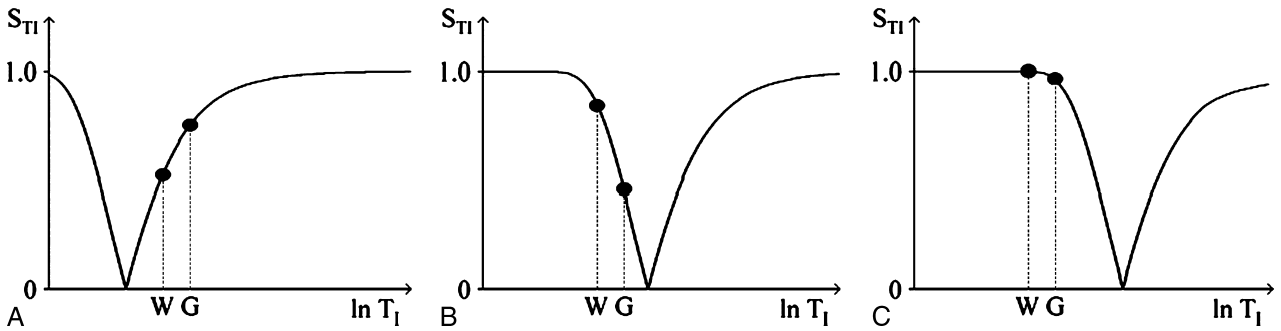


FIGURE 10. Plots of S_{T1} against $\ln T_1$ for short TI (A), medium TI (B), and long TI (C) for the long TR-IR sequence. The positions of the white (W) and gray matters (G) of the brain are shown. In (A) (the STIR sequence), the signal from the white matter is lower than that from the gray matter. In (B) (the medium TI sequence), the signal from the white matter is higher than that in the gray matter, and in (C) (the long TI, eg, T₂-FLAIR sequence), the signal from the white matter is slightly higher than that from the gray matter. These are the 3 main classes of the long TR-IR sequence.

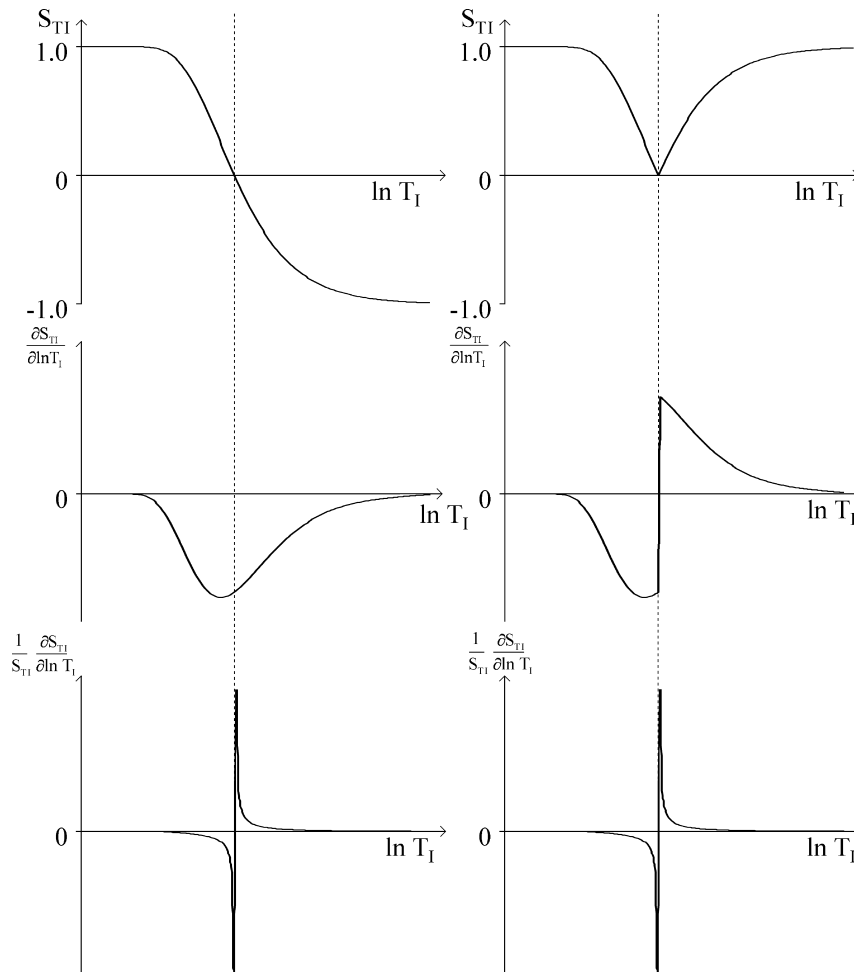


FIGURE 11. Plots of S_{T1} , $\frac{\partial S_{T1}}{\partial \ln T_1}$, and $\frac{1}{S_{T1}} \frac{\partial S_{T1}}{\partial \ln T_1}$ against $\ln T_1$ with phase-sensitive reconstruction (left column) and S_{T1} , $\frac{\partial S_{T1}}{\partial \ln T_1}$, and $\frac{1}{S_{T1}} \frac{\partial S_{T1}}{\partial \ln T_1}$ against $\ln T_1$ with magnitude reconstruction (right column; long TR-IR sequence). Null points are linked vertically. Note that the normalized partial derivatives (bottom row) becomes infinite at the null point.

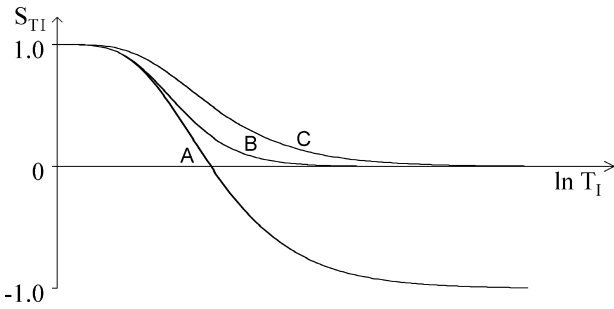


FIGURE 12. Plots of S_{T_1} against $\ln T_1$ for the long TR-IR sequence (phase-sensitive reconstruction) (A), the BIR sequence (B), and the SE sequence with TR equal to the T_1 used previously (C). The slope of the curves decreases from A to B to C, corresponding to a decrease in weighting.

The signal equation of the BIR sequence is

$$S_{BIR} = \left(1 - e^{-\frac{T_1}{T_1}}\right)^2 \quad [12]$$

The sequence weightings for absolute and fractional contrasts are

$$sW_{T_1/BIR/C_{ab}} = -k^{\frac{T_1}{T_1}} \left(1 - e^{-\frac{T_1}{T_1}}\right) e^{-\frac{T_1}{T_1}} \quad \text{and} \quad [13]$$

$$-2 \frac{T_1}{T_1} \cdot \frac{e^{-\frac{T_1}{T_1}}}{1 - e^{-\frac{T_1}{T_1}}}$$

The full signal equation of the IR sequence also includes the contributions from ρ_m and T_2 , as outlined for the SE sequence. The overall pattern can be represented in a similar way to Figure 8 but with the use of the BIR S_{T_1} filter rather than the SE S_{T_1} filter.

Signal for the double inversion recovery sequence as used for nulling both the white matter and the CSF,¹² which shows high contrast for small increases in the T_1 of white and gray matter, is seen in Figure 13.

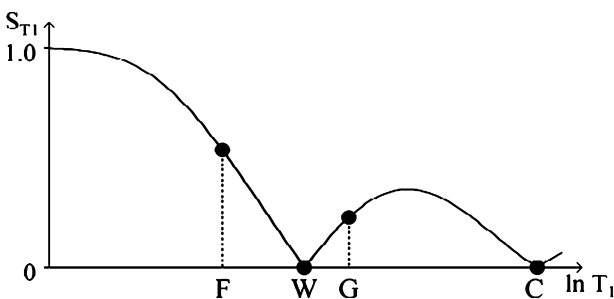


FIGURE 13. Double inversion recovery sequence. S_{T_1} is plotted against $\ln T_1$ for fat (F), white matter (W), gray matter (G), and CSF (C). Both the white matter and the CSF are nulled. For small increases in the T_1 of the white and gray matter, there is an increase in signal that is additive with any concurrent increases in ρ_m and T_2 , resulting in high contrast.

The Pulsed Gradient SE Sequence

This sequence is used to obtain D^* -weighted images. The signal equations are those of the basic SE sequence (Equations 1 and 2) multiplied by a fourth filter, S_{D^*} given by

$$S_{D^*} = e^{-bD^*}, \quad [14]$$

where b is the diffusion sensitivity parameter and D^* is the apparent diffusion coefficient. The pulsed gradient SE (PGSE) sequence uses gradient pulses on either side of the 180-degree pulse to sensitize the sequence to diffusion. The b value for such a sequence is given by $b = \gamma^2 G^2 \delta^2 \left(\Delta - \frac{\delta}{3}\right)$, where γ is the gyromagnetic ratio, G is the gradient strength, δ is the duration of the sensitizing pulses, and Δ is the separation between them. A useful approximation is to consider the situation where the gradient is on continuously, when b would equal $\frac{\gamma^2 G^2 TE^3}{12}$. In this situation (which is close to that often used clinically for maximum b value images), the diffusion sensitivity depends on TE. As a result, we have a single-pulse sequence parameter TE that affects both the T_2 and the D^* weighting.

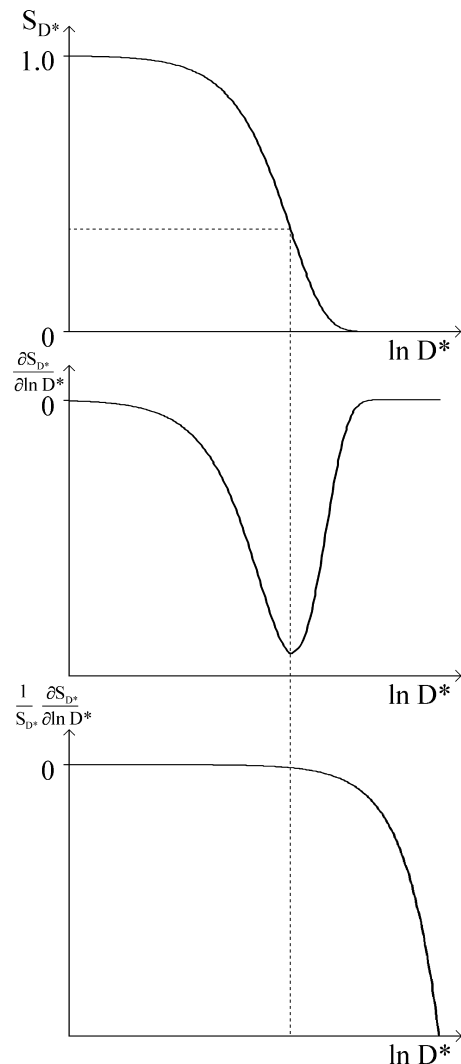


FIGURE 14. Plots of S_{D^*} , $\frac{\partial S_{D^*}}{\partial \ln D^*}$, and $\frac{1}{S_{D^*}} \frac{\partial S_{D^*}}{\partial \ln D^*}$ against $\ln D^*$ for the PGSE sequence. S_{D^*} is an exponential function. The partial derivative shows a minimum at $bD^* = 1$ (vertical dotted line).

The diffusion filter is shown in Figure 14. It is a negative exponential but has a shape similar to that of the SE T_1 filter as a consequence of the logarithmic scaling of the x -axis. The contrast is negative, and it is opposed to that for TE. The first partial derivative shows that weighting goes through a maximum at $bD^* = 1$. With increasing TE, the curve is shifted to the left that is opposite to that for the SE T_2 filters. The signal from both the T_2 and D^* filters decreases while TE is increased. With a typical D^* -weighted sequence ($SE_{TR/TE} = 5000/150$ ms, $b = 1000$ s/mm²), as that used to examine brain with $T_1 = 1000$ ms, $T_2 = 80$ ms, and D^* (gray) = 0.7×10^{-3} mm²/s, the sequence weighting ratio is given by

$$sW_{PGSE}(\rho_m:T_1:T_2:D^*) = \left(1 : -\frac{TR}{T_1} \frac{e^{-\frac{TR}{T_1}}}{1 - e^{-\frac{TR}{T_1}}} : \frac{TE}{T_2} : -bD^* \right) = (31 : -1.46 : -22) \quad [15]$$

Although such a sequence is usually described as diffusion weighted using the qualitative approach, the dominant sequence weighting is actually from T_2 (46%) compared with the -22% for diffusion. The T_2 and D^* weightings are opposed (ie, they are of opposite sign). In acute or hyperacute infarction during the initial phase, only D^* may change (with a decrease, ie, negative $\frac{\Delta D^*}{D^*}$). This can be modeled with the univariate signal approach. Because of the negative D^* sequence weighting and negative $\frac{\Delta D^*}{D^*}$, this results in a high signal. Over time, T_2 usually increases, and this change contributes to contrast, making the multivariate model necessary (Figs. 15 and 16). It may not be obvious which of D^* or T_2 is contributing most to contrast. In the later stages of infarction, D^* usually increases, resulting in contrast opposed to that produced by T_2 . This D^* weighting is usually dominated by the T_2 weighting, resulting in a high signal relative to a normal brain. D^* maps may help by showing actual values of D^* , providing that the image signal level is adequate to allow calculation of reliable values.

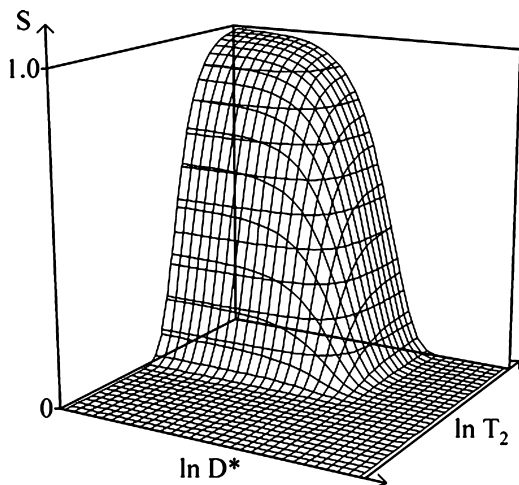


FIGURE 15. Three-dimensional plot of S against $\ln D^*$ along the x -axis and S against $\ln T_2$ along the y -axis. S is shown vertically along the z -axis. Detectable signal is seen at lower values of D^* and at longer values of $\ln T_2$. Signal is low or zero at higher values of D^* and shorter values of T_2 .

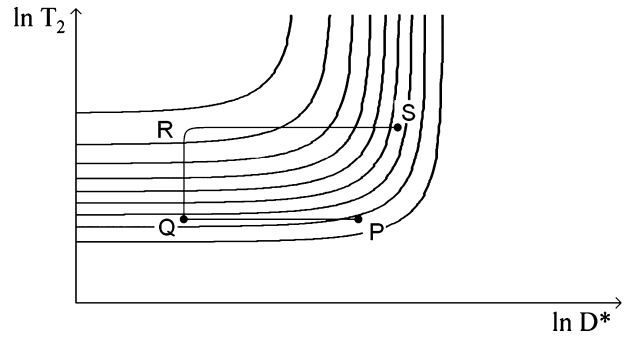


FIGURE 16. Plot of $\ln T_2$ against $\ln D^*$ with contours at different horizontal levels (from Fig. 15). A trajectory for acute cerebral infarction starting at P is shown moving horizontally to the left to Q (reduced D^*), with subsequent movement vertically to R (increasing T_2) and horizontally to the right to S (increasing D^*). The signal at point P is lower than that at point Q.

The sequence weightings are

$$sW_{D^*/PGSE/C_{ab}} = -bD^* e^{-bD^*} \quad sW_{D^*/PGSE/C_{fr}} = -bD^* \quad [16]$$

Diffusion-weighted sequences are frequently used with echo planar imaging data collections. These can be modeled using TE_{eff} . They also usually include a $b = 0$ (or in practice, approximately 5 s/mm²) sequence that has an S_{D^*} filter that is essentially flat and equal to 1.

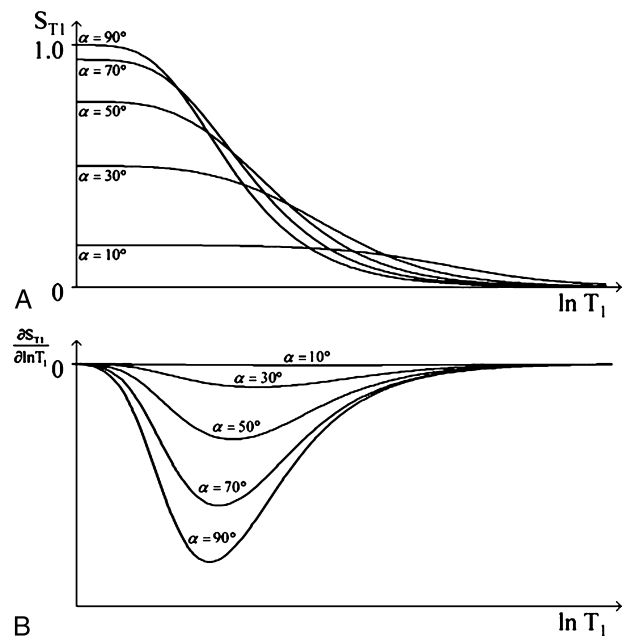


FIGURE 17. Plots of S_{T_1} (A) and $\frac{\partial S_{T_1}}{\partial \ln T_1}$ (B) against $\ln T_1$ for flip angles (α) of 90, 70, 50, 30, and 10 degrees for the SGE sequence. As the flip angle is decreased from 90 degrees $\ln(A)$, the slope of the curve on the left decreases. At 10 degrees, the curve is flat over an extensive region on the left. (B) shows the weighting. As the flip angle decreases from 90 degrees, the magnitude of the weighting decreases and the value of T_1 for maximum weighting increases.

The Spoiled Gradient Echo Sequence

Gradient-echo sequences can be divided into (1) spoiled gradient-echo (SGE), (2) steady state with free induction decay sampling, (3) steady state with SE sampling, and (4) balanced steady state free precession (bSSFP), although different systems of classification are used.¹³⁻¹⁶ In this section, the SGE sequence¹⁷⁻¹⁹ is considered, and in the next section, the bSSFP sequence is described. For the SGE sequences, the signal for the S_{T_1} filter is similar to that for the SE equation with the addition of a flip angle (α) term so that

$$S_{T_1} = \frac{k' \sin \alpha}{1 - \cos \alpha e^{-\frac{TR}{T_1}}} \left(1 - e^{-\frac{TR}{T_1}} \right). \quad [17]$$

The filters for flip angles of 90, 70, 50, 30, and 10 degrees for a given TR are shown in Figure 17. As the flip angle decreases, the signal and the slope decrease on the left, although signal may increase on the right. The slope of the curve is shown in Figure 17 where it goes through a maximum. These curves can be displayed parallel to the x ($\ln T_1$) axis in a 3-dimensional form as in Figure 18. Along lines parallel to the flip angle (α) axis (the y -axis), there is a maximum signal for a given T_1 . This is obtained by putting $\frac{\partial S}{\partial \alpha} = 0$, which gives the Ernst angle for maximum signal α_S , where

$$\cos \alpha_S = e^{-\frac{TR}{T_1}}. \quad [18]$$

The flip angle for maximum contrast, α_C , is obtained by putting $\frac{\partial S}{\partial \ln T_1 \partial \alpha} = 0$ for which

$$\cos \alpha_C = \frac{2e^{-\frac{TR}{T_1}} - 1}{1 - 2e^{-\frac{TR}{T_1}}} e^{-\frac{TR}{T_1}}. \quad [19]$$

Plots of α_S and α_C are shown in Figure 19 where the flip angle for maximum contrast is greater than that for maximum signal. For given values of T_1 and TR, Figure 19 provides values of flip angles to maximize contrast or signal.

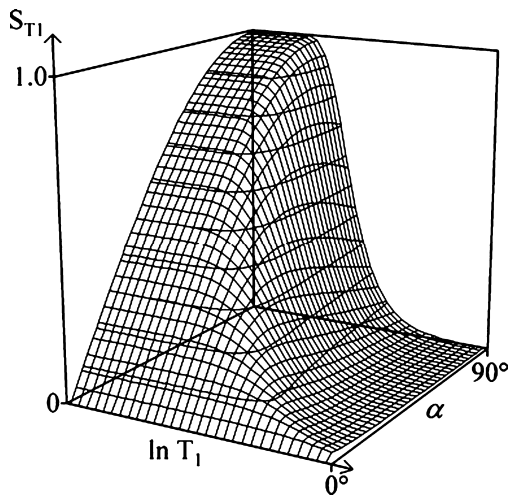


FIGURE 18. Plots of S_{T_1} against $\ln T_1$ along the x -axis and S_{T_1} against α along the y -axis with S_{T_1} vertically along the z -axis for the SGE sequence. The plots of S_{T_1} against $\ln T_1$ parallel to the x -axis shows variation in S_{T_1} with $\ln T_1$ at constant flip angle as in Figure 16A. The plots parallel to the y -axis (α) represent S_{T_1} plotted against α , with the maximum signal $\cos \alpha_S = e^{-\frac{TR}{T_1}}$, the Ernst angle.

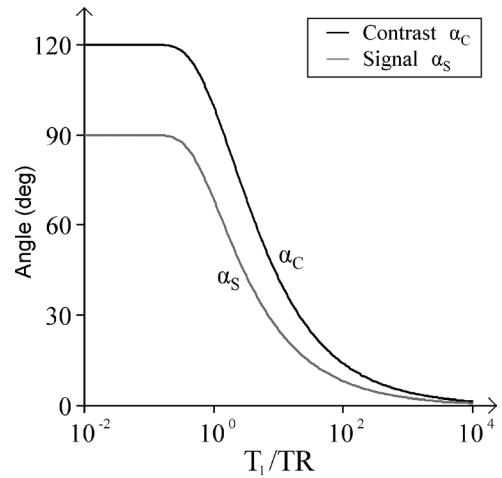


FIGURE 19. Plots of α_S (flip angle for maximum signal) and α_C (flip angle for maximum contrast) against $\frac{TR}{T_1}$ for the SGE sequence. This curve gives values of $\frac{TR}{T_1}$ to maximize signal and contrast. The flip angle for maximum contrast (α_C) is greater or equal to that for maximum signal (α_S). The curves reach a maximum on the left with low values of $\frac{TR}{T_1}$. At high values of $\frac{TR}{T_1}$, the flip angles for maximum signal and maximum contrast converge.

The effect of susceptibility and B_0 inhomogeneity in a voxel can be represented by

$$\frac{1}{T_2^*} = \frac{1}{T_2} + \gamma \Delta B, \quad [20]$$

where $\gamma \Delta B$ is the field inhomogeneity of the voxel under consideration due to B_0 inhomogeneity or susceptibility differences. This results in a fractional shortening of T_2 given by

$$\frac{\Delta T_2}{T_2} = \frac{-\gamma \Delta B T_2}{1 + \gamma \Delta B T_2}. \quad [21]$$

The fractional shortening increases with field inhomogeneity and with T_2 . It can be represented along the x -axis of the S_{T_2} curve.

The SGE sequence is also sensitive to chemical shift phase effects. The signal seen from protons in fat and water is the complex sum of the 2 contributions and includes phase differences developing over time TE. The signal may be represented with filters of ρ_m , T_1 , and T_2 for each of the water and

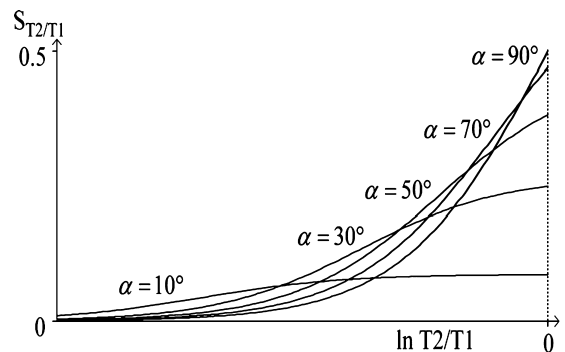


FIGURE 20. Sequence of SSFP. Plot of S_{T_2/T_1} against $\ln T_2/T_1$ for flip angles of 90, 70, 50, 30, and 10 degrees. For each flip angle, the signal increases with $\ln T_2/T_1$.

fat components by adding them in the complex domain using a phase filter with a phase difference φ given by

$$\phi = \gamma\delta \text{Bo TE}, \quad [22]$$

where δ is the chemical shift between the 2 components.

The bSSFP Sequence

The bSSFP sequence balances gradient areas in all 3 axes over TR and produces a signal that is the sum of free induction decay and SE contributions.^{13,14} Here, the signal equation with alternating sign RF pulses is used with some simplifications. Signal is a function of $\frac{T_2}{T_1}$ and can be represented for different flip angles as shown in Figure 20.¹⁵

Weighting is shown in Figure 21 for the $\frac{T_2}{T_1}$ component. The flip angle for maximum signal (α_s) is given by

$$\cos \alpha_s = \frac{1 - \frac{T_2}{T_1}}{1 + \frac{T_2}{T_1}}, \quad [23]$$

and that for maximum contrast α_c , by

$$\cos \alpha_c = \frac{1 - 3\frac{T_2}{T_1}}{1 + 3\frac{T_2}{T_1}}. \quad [24]$$

These are illustrated in Figure 22. For the common changes in disease where T_1 and T_2 both increase, the ratio $\frac{T_2}{T_1}$ may show relatively little change, and this may result in low intrinsic contrast.

Magnetization Preparation Filters

Pulse sequences can be regarded as consisting of preparation, excitation, and data acquisition periods. There may also be a postacquisition period, and each of these can have TP filters associated with them. Forms of magnetization preparation (MP) affecting the first period do not include acquisition modules and so are used in conjunction with pulse sequences that do have them. The magnetization properties usually effect contrast and weighting. Examples include saturation bands, fat saturation, and black blood preparation.

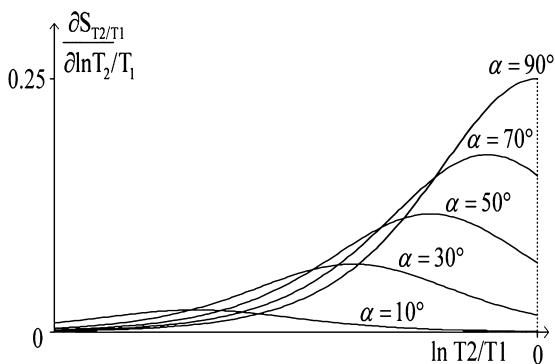


FIGURE 21. Sequence of bSSFP. Plot of $\frac{\partial S_{T_2/T_1}}{\partial \ln T_2/T_1}$ against $\ln T_2/T_1$. For each flip angle, the weighting is maximum at a value of $\ln \frac{T_2}{T_1}$

given by $\cos \alpha_c = \frac{1 - \frac{3T_2}{T_1}}{1 + \frac{3T_2}{T_1}}$. These progressively increase.

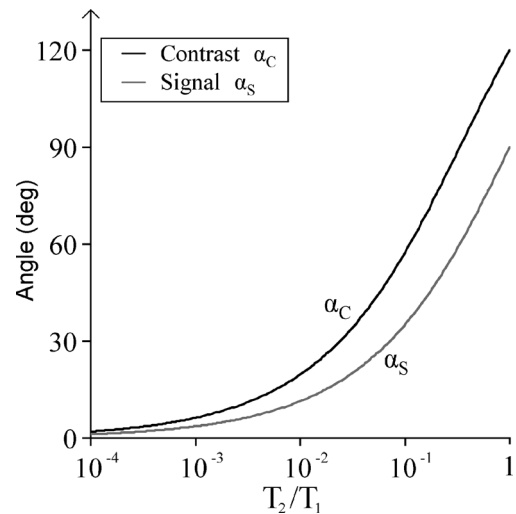


FIGURE 22. Flip angles of bSSFP for maximum signal and contrast. Plot of flip angle for maximum contrast α_c and maximum signal α_s against $\ln \frac{T_2}{T_1}$. The flip angle for maximum contrast is greater than that for maximum signal.

There is overlap with pulse sequences, and an inversion pulse may be regarded both as a form of MP and as part of a full pulse sequence as with the MP with rapid acquisition gradient echo sequence that has contrast similarities to the shorter TR-IR group of sequences. The effects on contrast and weighting can often be represented by simple filters or be modeled as pulse sequences.

Magnetization transfer can be regarded as a form of MP that decreases the observed ρ_m and the observed T_1 .^{20,21} Those effects can be represented on the x -axes of the S_{pm} and S_{T1} filters, respectively.

Acquisition Filters

These are filters that apply between the beginning and the end of data acquisition and are manifest as changes in signal in k -space and as a convolution in image space. They include T_2 filters, J-coupling, and T_1 filters such as that in the k -space reordered by TI at each slice position sequence.²²

With the fast SE sequence, higher signals acquired at shorter TEs are often mapped to the center of k -space and lower signals acquired at longer TEs are mapped to the periphery of k -space, resulting in a loss of edge definition. In addition with the fast SE sequence, the multiple inversion recovery pulses produce a degree of spin lock and a reduction in the J-coupling of lipid peaks so that they tend to coalesce. This reduces the interference effect between the peaks and increases the observed T_2 resulting in higher signal for fat relative to other tissues.²³ This typically becomes more apparent at longer TEs. The k -space reordered by TI at each slice position sequence maps data acquired at or around the null point to the center of k -space with data signal on either side of this point relatively decreased. This results in an edge enhancement effect in image space.²²

Postacquisition Filters

Many postacquisition procedures are possible involving single images or groups of images with contrast between voxels on the same or different images. A postacquisition filter of interest is subtraction of a later echo image from the first as used

with UTE sequences to selectively highlight short T_2 tissue components. This results in a band pass filter.⁵ The T_2 weighting functions show positive, zero or near-zero, and negative weighting. Different contrast may result from (1) an increase in T_2 so that signal enters the pass region of the filter, (2) an increase in T_2 within the pass region, and (3) an increase in T_2 so that the tissue leaves the pass region.

Changes in Tissue Properties in Disease

In the previous section, the main emphasis has been on sequence weighting, but as explained, image weighting is sequence weighting multiplied by fractional change in TP. These later changes are the subject of this section.

The most common change in the TP in disease is an increase in ρ_m , T_1 , and T_2 (and D^*) with the fractional change in the latter properties being greater than that in ρ_m . This is typically seen in acute infection, acute inflammation, edema, and many tumors. Reductions in tissue properties are less commonly seen in disease, but they occur in important conditions, including acute hemorrhage and acute infarction (D^*). A reduction in T_1 and T_2 may also be seen with an accumulation of paramagnetic material. Many tumors display a decrease in D^* .

Contrast Agents

Contrast agents also change tissue properties including T_1 and T_2 and susceptibility. They reduce T_1 and T_2 as shown in Equations 26 and 27, respectively. With pulse sequences designed to maximize T_1 or T_2 weighting and minimize T_2 or T_1 weighting respectively, we can use the univariate model (assuming $\frac{\Delta\rho_m}{\rho_m} = 0$ when comparing images before and after enhancement).

The effect of a contrast agent such as gadolinium chelate on T_1 and T_2 is given by

$$1/T_{1c} = 1/T_{1b} + r_1c \tag{25}$$

and

$$1/T_{2c} = 1/T_{2b} + r_2c, \tag{26}$$

where r_1 and r_2 are the T_1 and T_2 relaxivities and c is the concentration of the contrast agent. The subscript b indicates baseline, and the subscript c indicates contrast enhanced.

The image weightings for the T_1 and T_2 filters of an SE sequence, for example, are the sequence weightings multiplied by the fractional changes in T_{1b} or T_{2b} :

$$\frac{\Delta T_1}{T_{1b}} = \frac{-r_1cT_{1b}}{1 + r_1cT_{1b}} \tag{27}$$

and/or

$$\frac{\Delta T_2}{T_{2b}} = \frac{-r_2cT_{2b}}{1 + r_2cT_{2b}} \tag{28}$$

Noise

So far, we have mainly considered signal and contrast, but these are always accompanied by noise, and both the signal level at which contrast is produced and the background noise are of critical importance. The signal-to-noise ratio (SNR) is an important index of machine performance and sets an upper limit on contrast-to-noise ratio (CNR). The SNR is also important in the low signal situation where normalization of the signal and weighting ratios become invalid.

The CNR is related to the detectability of differences because these are seen against the background noise. It is usual to compare absolute contrast to noise on the grounds that the noise and signal are scaled together so that this represents a form of

normalization and improves the validity of comparisons. C_{fr} is scaled relative to tissue signals. The image noise level reflects voxel size, time of acquisition, bandwidth, coil performance, and other factors⁹ and is usually regarded as uniformly distributed throughout the image, although this may not be true of images obtained with partially parallel techniques. Weighting is concerned with the origin of contrast from changes or differences in tissue properties, whereas CNR is concerned with detectability of that contrast.

Signal and Contrast Strategies

The emphasis with weighting is on intrinsic contrast (differences with respect to normal in a single tissue), although it includes extrinsic contrast (differences between 2 or more different tissues or fluids). The main interest is in maximizing contrast or weighting that often requires minimizing opposed contrast or weighting. There are other MR imaging strategies including maximizing extrinsic contrast where maximizing signal from a tissue may be the key. This is often achieved when the intrinsic contrast for that tissue is zero. Another strategy is to make the weighting for several different tissue properties additive as with the magnitude-reconstructed STIR sequence. The SNR and the CNR per unit time (or the square root of time) may provide meaningful measures of imaging efficiency.

Other Types of Weighting

We have concentrated on the main types of weighting seen clinically, but there are now 30 to 40 different types of weighting described in the English language imaging literature. These often follow directly from the Bloch equations (as for ρ_m , T_1 , and T_2 above) or are linked to them with a specific relationship (as with contrast agents). There is also a third class with less well-defined changes where the sequence weighting or change in tissue properties or both are not fully characterized and weighting is appropriately described in qualitative terms.

Issues

It may not be clear which of C_{ab} or C_{fr} is most appropriate to describe contrast. Contrast may also be influenced by the window width and level chosen to display the image. Finally, a continuous approach has been used in this article to explain contrast based on small changes, but a discrete approach can also be used, and this may be more appropriate for large changes or differences.

CONCLUSIONS

The filters formulation provides a graphic and mathematical representation of weighting. The univariate model shows the TP values where weighting and contrast are maximized and defines areas where weighting is minimal or absent. It shows that values of T_1 or T_2 greater than these for maximum weighting may produce significant contrast and so may T_1 or T_2 values less than those that produce maximum weighting. It is possible to estimate weighting relative to the maximum value using basic calculations and to determine signal levels at which this is achieved. It encompasses both absolute and fractional contrast, although the later is problematic at zero or near-zero signal levels. This approach includes both sequence and imaging weighting. It also covers the full range of clinical values of ρ_m , T_1 , and T_2 so that regions with different weightings can be readily recognized.

The multivariate model gives a quantitative estimate of the different contributions of each TP to the total image weighting. It extends the concept of weighting from qualitatively designating one TP as the dominant source of contrast to including all tissue properties, providing a quantitative measure of each of

their relative contributions to weighting, attributing a sign to each contribution and doing this for both sequence and image weighting.

The same general concepts apply to SE, IR, PGSE, SGE, and bSSFP sequences. The different classes of the long TR-IR sequence can be characterized, as well as those of the shorter TR-BIR/T₁-FLAIR sequence. With the PGSE sequence, T₂ weighting is often greater than D* weighting and different patterns of contrast may be observed with T₂ and D* weighting additive or opposed with different diseases and at different stages of disease. With SGE and bSSFP sequences, the flip angles for maximizing signal and contrast can be calculated.

For common sequences and images in clinical use, it is possible to construct graphic signatures to show the signal, contrast, and weighting of all tissues or fluids visualized with a sequence and to use the corresponding mathematical formulation to quantitatively compare different sequences and images. The approach helps resolve many of the anomalies and apparent contradictions associated with the qualitative approach and leads to insights that are not otherwise apparent.

This approach is based on the use of partial derivatives of the logarithm of tissue properties and explicit definitions of sequence and image weightings. Partial derivatives were used to estimate CNRs in 1983²⁴ and as a basis for calculating the equivalent of sequence weighting using a linear (rather than a logarithmic) TP scale in 1984.²⁵ Elster²⁶ derived parameter weighting indices that are essentially the same as sequence weighting ratios in 1988 for SE and IR sequences. The partial derivative approach has also been applied to SGE sequences to calculate sequence contrast.^{17,18}

ACKNOWLEDGMENTS

We wish to acknowledge extensive help with the manuscript from Anne Rauh and Zach Smith.

REFERENCES

1. Axel L. Revised glossary of MR terms. *Radiology*. 1987;162:874.
2. Elster AD, Burdette JH. *Questions and Answers in Magnetic Resonance Imaging*. 2nd ed. St Louis, MO: Mosby; 2001:100.
3. Parker DL, Tsuruda JS, Goodrich KC, et al. Contrast-enhanced magnetic resonance angiography of cerebral arteries. A review. *Invest Radiol*. 1998;33:560–572.
4. Reichert IL, Robson MD, Gatehouse PD, et al. Magnetic resonance imaging of cortical bone with ultrashort TE pulse sequences. *Magn Reson Imaging*. 2005;23:611–618.
5. Robson MD, Gatehouse PD, Bydder M, et al. Magnetic resonance: an introduction to ultrashort TE (UTE) imaging. *J Comput Assist Tomogr*. 2003;27:825–846.
6. Bottomley PA, Foster TH, Argersinger RE, et al. A review of normal tissue hydrogen NMR relaxation times and relaxation mechanisms from 1–100 MHz: dependence on tissue type, NMR frequency, temperature, species, excision, and age. *Med Phys*. 1984;11:425–448.
7. Rooney WD, Johnson G, Li X, et al. Magnetic field and tissue dependencies of human brain longitudinal ¹H₂O relaxation in vivo. *Magn Reson Med*. 2007;57:308–318.
8. Busse RF, Hariharan H, Vu A, et al. Fast spin echo sequences with very long echo trains: design of variable refocusing flip angle schedules and generation of clinical T2 contrast. *Magn Reson Med*. 2006;55:1030–1037.
9. Hendrick RE. Contrast and image noise. In: Stark DD, Bradley WG, eds. *Magnetic Resonance Imaging*. 3rd ed. St Louis, MO: Mosby; 1999:43–67.
10. Bydder GM, Young IR. MR Imaging: clinical use of the inversion recovery sequence. *J Comput Assist Tomogr*. 1985;9:659–675.
11. Melhem ER, Israel DA, Eustace S, et al. MR of the spine with a fast T₁-weighted fluid-attenuated inversion recovery sequence. *AJNR Am J Neuroradiol*. 1997;18:447–454.
12. Redpath TW, Smith FW. Technical note: use of a double inversion recovery pulse sequence to image selectively grey or white brain matter. *Br J Radiol*. 1994;67:1258–1263.
13. Elster AD. Gradient echo MR imaging: techniques and acronyms. *Radiology*. 1993;186:1–8.
14. Scheffler K, Lehnhardt S. Principles and applications of balanced SSFP techniques. *Eur Radiol*. 2003;13:2409–2418.
15. Bernstein MA, King KF, Zhou XJ. *Handbook of MRI Pulse Sequences*. Amsterdam, the Netherlands: Elsevier; 2004:p. 596.
16. McRobbie DW, Moore EA, Graves MJ, et al. *MRI From Picture to Proton*. 2nd ed. Cambridge, UK: Cambridge University Press; 2007:236–257.
17. Buxton RB, Edelman RR, Rosen BR, et al. Contrast in rapid MR imaging: T₁- and T₂-weighted imaging. *J Comput Assist Tomogr*. 1987;11:7–16.
18. Pelc NJ. Optimization of flip angle for T₁ dependent contrast in MRI. *Magn Reson Med*. 1993;29:695–699.
19. Neelavalli J, Haacke EM. A simplified formula for T(1) contrast optimization for short-TR steady-state incoherent (spoiled) gradient echo sequences. *Magn Reson Imaging*. 2007;25:1397–1401.
20. Henkelman RM, Stanisz GJ, Graham SJ. Magnetization transfer in MRI: a review. *NMR Biomed*. 2001;14:57–64.
21. Hajnal JV, Baudouin CJ, Oatridge A, et al. Design and implementation of magnetization transfer pulse sequences for clinical use. *J Comput Assist Tomogr*. 1992;16:7–18.
22. Oatridge A, Curati WL, Herlihy AH, et al. Evaluation of a FLAIR sequence designed to reduce CSF and blood flow artifacts by use of k-space reordered by inversion time at each slice position (KRISP) in high grade gliomas of the brain. *J Comput Assist Tomogr*. 2001;25:251–256.
23. Henkelman RM, Hardy PA, Bishop JE, et al. Why fat is bright in RARE and fast spin-echo imaging. *J Magn Reson Imaging*. 1992;2:533–540.
24. Edelstein WA, Bottomley PA, Hart HR, et al. Signal, noise and contrast in nuclear magnetic resonance (NMR) imaging. *J Comput Assist Tomogr*. 1983;7:391–401.
25. Kurtz D, Dwyer A. Isosignal contours and signal gradients as an aid to choosing MR imaging techniques. *J Comput Assist Tomogr*. 1984;8:819–828.
26. Elster AD. An index system for comparative parameter weighting in MR imaging. *J Comput Assist Tomogr*. 1988;12:130–134.